UDC 621.391.28(075)

A. Kokhanov, DSc., Assoc. Prof.
Odessa Polytechnic National University, 1 Shevchenko Ave., Odesa, Ukraine, 65044, E-mail: okokhanov@gmail.com

FORMATION OF A SIGNAL WITH HARTLEY AMPLITUDE-PHASE MODULATION AS THE SUM OF TWO SIGNALS WITH HARTLEY AMPLITUDE MODULATION

О. Коханов. **Формування сигналу з амплітудно-фазовою модуляцією Хартлі як суми двох сигналів з амплітудною модуляцією Хартлі.** У роботі наводиться результат проведених досліджень, в результаті якого розроблено теоретичне обґрунтування нового виду модуляції – амплітудно-фазової модуляції Хартлі. Цей тип модуляції має додаткову несучу, яка є ортогональною по відношенню до відомої амплітудно-фазової модуляції. За такої умови, синфазна та квадратурна складові амплітудно-фазової модуляції Хартлі є амплітудними модуляціями Хартлі, причому, амплітудна модуляція Хартлі квадратурного каналу (квадратурна складова) є ортогональною амплітудною модуляцією Хартлі відносно синфазного каналу. Це також дозволяє сформувати сигнал амплітудно-фазовой модуляції Хартлі з квадратним сузір'ям – квадратурною модуляцією Хартлі. В роботі розглянуто також спосіб демодуляції сигналу з амплітудно-фазовою модуляцією Хартлі з використанням синхронного детектора. Показано, що сигнал з амплітудно-фазовою модуляцією Хартлі має підвищену завадостійкість до шуму в каналі зв'язку у порівнянні з відомою амплітудно-фазовою модуляцією. У роботі також наведено порівняння властивостей сигналів з квадратурною модуляцією Хартлі і відомого сигналу із квадратурною модуляцією. Показано, що енергетичний виграш сигналу з квадратурною модуляції Хартлі у порівнянні з квадратурною модуляцією, становить 6 дБ. Крім того, квадратурна модуляція Хартлі має таке ж саме значення середнього значення енергії, що припадає на один символ як і сигнали з КАМ модуляцією. У роботі наведено висновок аналітичного виразу для розрахунку відношення сигнал-шум для сигналу з квадратурної модуляції Хартлі. Показано, що отримані теоретичні результати для обчислення похибки помилково прийнятого символу добре погоджуються з отриманими результатами імітаційного моделювання. Наводиться порівняння одержаних результатів імітаційного моделювання при обчисленні значень для обчислення похибки помилково прийнятого символу для сигналів з квадратурною модуляцією Хартлі и відомою квадратурною модуляцією.

Ключові слова: амплітудна модуляція Хартлі, амплітудно-фазова модуляція Хартлі, модуляція сигналу, демодуляція сигналу, помилки прийнятого сигналу, середнє значення енергії

A. Kokhanov. **Formation of a signal with Hartley amplitude-phase modulation as the sum of two signals with Hartley amplitude modulation.** The paper presents the results of the research, which outcome in the development of a theoretical justification for a new type of modulation – Hartley amplitude-phase modulation. This type of modulation has an additional carrier that is orthogonal to the known amplitude-phase modulation. Moreover, the in-phase and quadrature components of the Hartley amplitude-phase modulation are Hartley amplitude modulations, and the Hartley amplitude modulation of the quadrature channel (the quadrature component) is an orthogonal Hartley amplitude modulation with respect to the in-phase channel. This also allows the formation of a Hartley amplitude-phase modulation signal with a square constellation - quadrature Hartley modulation. The paper also considers a method of demodulating a signal with Hartley amplitude-phase modulation using a synchronous detector. It is shown that a signal with Hartley amplitude-phase modulation has increased immunity to noise in the communication channel compared to the known amplitude-phase modulation. The paper also compares the properties of signals with quadrature Hartley modulation and a known signal with quadrature modulation. It is shown that the energy gain of a signal with quadrature Hartley modulation compared to quadrature modulation is 6 dB. In addition, quadrature Hartley modulation has the same average energy value per symbol as signals with QAM modulation. The paper presents the derivation of an analytical expression for calculating the signal-to-noise ratio for a signal from quadrature Hartley modulation. It is shown that the obtained theoretical results for calculating the error of a falsely received symbol agree well with the obtained results of simulation modeling. A comparison of the obtained simulation results when calculating the values for calculating the error of an erroneously received symbol for signals with Hartley quadrature modulation and known quadrature modulation is presented.

Keywords: Hartley amplitude modulation, Hartley amplitude-phase modulation, signal modulation, signal demodulation, errors of the received signal, average energy value

1. Introduction

Amplitude modulation (AM) [1 – 6] was recommended by the International Telecommunication Union (ITU) for limited use in radio communication systems due to its low efficiency. $\beta = 1$ It is known that the efficiency of amplitude modulation is 33% at the maximum modulation index. $\beta = 1$ In [7], Hartley amplitude modulation (HAM) is described, which provides signal transmission similar to the signal with amplitude modulation, but has an efficiency of 90% at the modulation index and with half the carrier frequency amplitude, which allows automatic frequency and phase adjustment systems to operate efficiently, as when using the well-known AM.

2. Literature review and problem statement

As shown in [8, p. 152], a signal with quadrature amplitude modulation (QAM) can be obtained by simultaneously transmitting two separate k-bit information blocks on two orthogonal carriers that

DOI: 10.15276/opu.1.71.2025.19

ISSN 2076-2429 (print)
ISSN 2223-3814 (online)

are in quadrature, that is, $\cos(2\pi f_0 t)$ and $\sin(2\pi f_0 t)$. In this case, the QAM signal can be represented by the sum of two modulated signals with balanced amplitude modulation (BAM, Doubly Site Band – DSB) [8, (4.3.19)] as:

$$S_m(t) = Re\,[(A_{mc} + jA_{ms})g(t)e^{J2\pi f_0 t}] = A_{mc}g(t)\cos(2\pi f_0 t) + jA_{ms}g(t)\sin(2\pi f_0 t), \quad (1)$$

where $m = 1,2,\ldots,M$ and $0 \le t \le T$, A_{mc} and A_{ms} are the information amplitudes of the signal for quadrature carriers, and $g(t)$ is the shaping pulse.

Another form of representation of the QAM signal [8, (4.3.20)] can be represented in the vector form:

$$S_m(t) = Re\,[(V_m e^{J\theta_m}\, g(t)e^{J2\pi f_0 t}] = V_m e^{J\theta_m}\, g(t)\cos(2\pi f_0 t + \theta_m), \quad (2)$$

where $V_m = \sqrt{A_{mc}^2 + A_{ms}^2}\,\theta_m = \operatorname{arctg}\dfrac{A_{mc}}{A_{ms}}$. Here, it can be noted that the signal with quadrature amplitude modulation (2) in this case can be generated using a combination of M_1-level QAM signal and M_2-positional phase modulation (PM), provided that the $M = M_1 M_2$ points of the state space [8, p. 151]. In this case, it should be noted that $m + n = \log_2(M_1 M_2)$ – is the number of binary symbols occurring at a rate of $R/(m+n)$, where R – is the bit rate of the bit stream. An example of a signal constellation for M = 8 amplitude-phase modulation (APM) is shown in Figure 1.

A signal with a square APM signal constellation is called quadrature amplitude modulation (QAM). For the case of QAM modulation, the signal can be represented as the sum of two orthonormalised signals [8, p. 152]:

$$S_m(t) = S_{m1} f_1(t) + S_{m2} f_2(t), \quad (3)$$

where $f_1(t) = \sqrt{\dfrac{2}{\varepsilon_g}}\, g(t)\cos(2\pi f_0 t)$, $f_2(t) = -\sqrt{\dfrac{2}{\varepsilon_g}}\, g(t)\sin(2\pi f_0 t)$, ε_g is the energy of the signal on the symbolic interval T, and:

$$S_m = [S_{m1}\, S_{m2}] = \left[A_{mc}\sqrt{\frac{1}{2}\varepsilon_g} \;\; A_{ms}\sqrt{\frac{1}{2}\varepsilon_g} \right]. \quad (4)$$

For rectangular signal constellations at $M = 2^k\sqrt{M} = 2^{k/2}$, where k is even, the QAM signal [8, p. 236] can be formed as the sum of two AM signals on quadrature carriers at $\sqrt{M} = 2^{k/2}$ signal points and half the power of these QAM signals. In this case:

$$S_m(t) = \frac{A_{mc}}{\sqrt{2}}\cos(2\pi f_0 t) + \frac{A_{ms}}{\sqrt{2}}\sin(2\pi f_0 t), \quad (5)$$

or

$$S_m(t) = A_m \cos(2\pi f_0 t) + B_m \sin(2\pi f_0 t), \quad (6)$$

where A_m and B_m are the in-phase and quadrature channel amplitudes, respectively, on the symbolic interval m.

3. The purpose of this paper is to obtain a theoretical justification of signal formation with Hartley amplitude-phase modulation and to identify its properties and differences from the known amplitude-phase modulation.

4. Amplitude-phase Hartley modulation

In [7], Hartley amplitude modulation is presented, which allows to provide high efficiency (90%) in the transmission of information compared to AM. There is also a description of Hartley Doubly Site Band (HDSB), which is an amplitude modulation of Hartley, but without a carrier frequency. The HBD signal can be represented by:

$$S_m(t) = A(t)\beta\cos\left(\frac{\pi}{4} - \omega_0 t - \varphi\right), \quad (7)$$

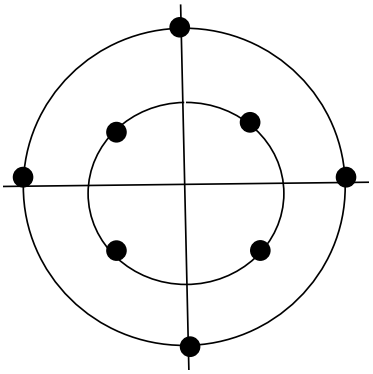

Fig. 1. An example of an AFM signal constellation for M = 8

where $A(t) = A_0 \cos(\Omega t + \Theta)$ is a modulating signal with frequency Ω, initial phase Θ, $\beta = A_m / A_0$, A_m is the maximum value of the modulating signal amplitude, A_0 is the carrier (modulated signal) amplitude, and φ is the initial phase of the carrier frequency.

The Hilbert-coupled signal of signal (7) is of the form [7]:

$$S_m(t) = A(t)\beta \sin\left(\frac{\pi}{4} - \omega_0 t - \varphi\right). \quad (8)$$

Thus, by analogy with the QAM signal (5) and (6), using (7) and (8), the expression for the Hartley Quadrature Amplitude Modulation (QAMH) signal can be written as:

$$S_m(t) = \frac{A_m}{\sqrt{2}} \cos\left(\frac{\pi}{4} - \omega_0 t - \varphi\right) + \frac{B_m}{\sqrt{2}} \sin\left(\frac{\pi}{4} - \omega_0 t - \varphi\right). \quad (9)$$

The signal (9) can also be represented as:

$$\begin{aligned} S_m(t) &= \frac{A_m}{\sqrt{2}} \cos(\omega_0 t + \varphi) + \frac{A_m}{\sqrt{2}} \sin(\omega_0 t + \varphi) + \frac{B_m}{\sqrt{2}} \cos(\omega_0 t + \varphi) - \frac{B_m}{\sqrt{2}} \sin(\omega_0 t + \varphi) = \\ &= \frac{A_m + B_m}{\sqrt{2}} \cos(\omega_0 t + \varphi) + \frac{A_m - B_m}{\sqrt{2}} \sin(\omega_0 t + \varphi). \end{aligned} \quad (10)$$

It can be seen from (10) that the QAMH signal can be generated in the same way as the well-known AM signal, but with the amplitude $\frac{A_m + B_m}{\sqrt{2}}$ in the in-phase channel and the amplitude $\frac{A_m - B_m}{\sqrt{2}}$ in the quadrature channel. The maximum value of the length of the QAMH amplitude vector in the square signal constellation will be at the equality of the values of the modules $|A_m| = |B_m|$, but $\sqrt{2}$ in the denominator in (10) reduces the value of the length of the amplitude vector to the same value as in the signal constellation of the known QAM signal, which allows us to assert the equality of the powers of the QAMH signal and the QAM signal at the same value of *M*. Thus, the dynamic ranges in the formation of the QAMH signal and the QAM signal will be equal, which makes it possible to use the same transmission systems for the transmission of information using QAMH signals as for the transmission of information using QAM signals. It also follows that the minimum distance between the symbols of the QAMH signal will be described by the same expression as for the QAM signal [9, p.119], i.e.:

$$d_E^2 = [(I_k - I_{k\pm1})^2 + (Q_k - Q_{k\pm1})^2]T_s, \quad (11)$$

where I_k and Q_k are the values of the amplitudes of the in-phase and quadrature components at the k-th symbolic interval with period T_s. For adjacent states [9, p.119], one of the terms in (11) is always zero, so that the distance between symbols is the difference of adjacent values of the quadrature or in-phase components multiplied by a dimensional factor.

With the normalizing factor equal to *U*, the distance between adjacent symbols (for a square constellation) will be equal to $d_E^2 = U^2 T_s / 2$ [9, p.119]. Figure 2 shows the structure of the signal constellation for AM 16, where $m = \log_2 M, M$, is the number of AM modulation levels. For $M = 16$, $m = 4$.

For the square signal constellation of the QAM 16 signal (Fig. 2), it is possible to determine the average power value per symbol [9, p.119]. For the state diagram shown in Fig. 2 (at the scale of symbol values $A_i = \{-1, -3, 1, 3\}$, $B_j = \{-1, -3, 1, 3\}$ there are three states of symbol energy: $P_1 = (3^2 + 3^2) = 4.24$; $P_2 = (1^2 + 3^2) = 3.16$; $P_3 = (1^2 + 1^2) = 1.14$.

Accordingly, in this case, the average energy per symbol can be defined as [10, p.120].

$$P_{QAM} = \frac{4P_1 + 8P_2 + 4P_3}{16} = \frac{16.96 + 25.28 + 4.56}{16} = 2.9575. \quad (12)$$

As can be seen from Fig.2, it is possible to write the expression for calculating the average energy per symbol for the AM modulation in general for an arbitrary value as $M = 2^{m+n}$ (*m* and *n* positive integers):

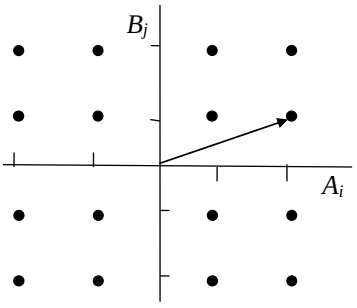

Fig. 2. Signal constellation (state diagram) of the QAM 16 signal

ISSN 2076-2429 (print)
ISSN 2223-3814 (online)

$$E_{sQAM} = \frac{1}{M}\sum_{i=1}^{m}\sum_{j}^{n}(A_i^2 + B_j^2)\,. \tag{13}$$

Taking into account the values of the amplitudes in (10) and taking into account (13), we can write the expression for determining the average energy per symbol for the QAMH modulation for an arbitrary value $M = 2^{m+n}$ as:

$$E_{sHQAM} = \frac{1}{M}\sum_{i=1}^{m}\sum_{j}^{n}\left[\left(\frac{A_i + B_j}{\sqrt{2}}\right)^2 + \left(\frac{A_i - B_j}{\sqrt{2}}\right)^2\right] = \frac{1}{M}\sum_{i=1}^{m}\sum_{j}^{n}(A_i^2 + B_j^2). \tag{14}$$

Comparing (13) and (14), it can be concluded that signals with QAMH have the same average energy per symbol as the QAM signal.

Thus, in the transmitting part of the system, the same transmitting equipment can be used to generate the QAMH signal as for the formation of the QAM signals, as follows from (10).

Demodulation of the AMF signal

Signal (10) is transmitted to the communication channel and then enters the receiver input (demodulator). It should be borne in mind that the power of additive white Gaussian noise (AWGN) in the communication channel $N(t) = n^2(t)$ is added to the AMF signal in the communication channel and divided in half between the quadrature and in-phase channels of the synchronous detector (where $n(t)$ is the noise amplitude of a random process) [7,10]. In the case of the presence of AWGN in the communication channel, the value of the noise amplitudes in the in-phase and quadrature channels can be written:

$$\sqrt{\frac{N(t)}{2}} = \frac{n(t)}{\sqrt{2}}\,. \tag{15}$$

The QAMH signal is demodulated using a synchronous quadrature demodulator. Since in synchronous detectors the signal phase and the phase of the reference oscillator are equalised by a phase-locked loop (PLL) system, you can set the value to $\varphi = 0$. In the in-phase channel of the QAMH demodulator, the signal (9) is multiplied with the signal of the reference quadrature oscillator $2\cos\omega_0 t$ and the output of the multiplier will be formed by the signal:

$$\begin{aligned} U_c &= \left\{\left[\frac{A_m}{\sqrt{2}}\cos\left(\frac{\pi}{4} - \omega_0 t\right) + \frac{B_m}{\sqrt{2}}\sin\left(\frac{\pi}{4} - \omega_0 t\right)\right] + n(t)/\sqrt{2}\right\}\cdot 2\cos\omega_0 t = \\ &= \left(\frac{A_m}{\sqrt{2}}\right)\cos\left(\frac{\pi}{4} - \omega_0 t + \omega_0 t\right) + \left(\frac{A_m}{\sqrt{2}}\right)\cos\left(\frac{\pi}{4} - \omega_0 t - \omega_0 t\right) + \\ &+ \left(\frac{B_m}{\sqrt{2}}\right)\sin\left(\frac{\pi}{4} - \omega_0 t + \omega_0 t\right) + \left(\frac{B_m}{\sqrt{2}}\right)\sin\left(\frac{\pi}{4} - \omega_0 t - \omega_0 t\right) + \sqrt{2}\,n(t)\cos\omega_0 t. \end{aligned} \tag{16}$$

In the quadrature channel of the QAMH demodulator, the signal (9) is multiplied with the signal $2\sin\omega_0 t$ of the quadrature oscillator, and the output of the multiplier will be generated as follows:

$$\begin{aligned} U_s &= \left\{\left[\frac{A_m}{\sqrt{2}}\cos\left(\frac{\pi}{4} - \omega_0 t\right) + \frac{B_m}{\sqrt{2}}\sin\left(\frac{\pi}{4} - \omega_0 t\right)\right] + n(t)/\sqrt{2}\right\}\cdot 2\sin\omega_0 t = \\ &= \left(\frac{A_m}{\sqrt{2}}\right)\sin\left(\omega_0 t + \frac{\pi}{4} - \omega_0 t\right) + \left(\frac{A_m}{\sqrt{2}}\right)\sin\left(\omega_0 t - \frac{\pi}{4} + \omega_0 t\right) + \\ &+ \left(\frac{B_m}{\sqrt{2}}\right)\cos\left(\omega_0 t - \frac{\pi}{4} + \omega_0 t\right) - \left(\frac{B_m}{\sqrt{2}}\right)\cos\left(\omega_0 t + \frac{\pi}{4} - \omega_0 t\right) + \sqrt{2}\,n(t)\sin\omega_0 t. \end{aligned} \tag{17}$$

It is known that the AWGN is characterised by the fact that its "values" of amplitudes at any two arbitrarily close moments of time $n(t)$ and $n(t)$ are uncorrelated [11, p. 110]. It is also known that the noise components $n(t)\cos\omega_0 t$ and $n(t)\sin\omega_0 t$ are random stationary processes, since their amplitudes are random variables, the average value of the processes themselves does not depend on time *t*, and their correlation function depends on only one variable [11, p. 111].

The quadrature channel, it should be noted, introduces into the noise amplitude $n(t)\cos\omega_0 t$ only a phase shift $\frac{\pi}{2}$ relative to the in-phase channel, which is equivalent to a time shift $n(t+\tau)\cos[\omega_0(t+\tau)] = n(t+\tau)\sin[\omega_0(t)]$ where $\omega_0\tau = \frac{\pi}{2}$, which does not change the nature of the random process. In addition, it is shown in [8, pp. 138–139; 12, p. 81, p. 84] that the quadrature processes $n(t)\cos\omega_0 t$ and $n(t)\sin\omega_0 t$ are normal and statistically independent.

After passing the signals (16) and (17) through low-pass filters with a cutoff frequency $\Omega = \frac{1}{T}$, where: T is the value of the symbolic interval, we obtain the signal at the output of the in-phase channel of the synchronous demodulator in the form:

$$U_1 = \frac{A_m}{\sqrt{2}}\cos\left(\frac{\pi}{4}\right) + \frac{B_m}{\sqrt{2}}\sin\left(\frac{\pi}{4}\right) + \sqrt{2}\,\hat{n}_c(t), \tag{18}$$

and the signal at the output of the filter of the quadrature channel of the synchronous demodulator will be in the form:

$$U_2 = \frac{A_m}{\sqrt{2}}\sin\left(\frac{\pi}{4}\right) - \frac{B_m}{\sqrt{2}}\cos\left(\frac{\pi}{4}\right) + \sqrt{2}\hat{n}_s(t), \tag{19}$$

where: $\hat{n}_c(t)$ is the amplitude of the noise (process) $n(t)\cos\omega_0 t$, after filtering in the in – phase channel and $\hat{n}_c(t)$ is the amplitude of the noise (process), $n(t)\sin\omega_0 t$ after filtering in the quadrature channel (which does not change the nature of random processes). It is assumed that the characteristics of the low-pass filters of the in-phase and quadrature channels of the synchronous detector of the QAMH signal are identical.

Summing the values of signals (18) and (19), we obtain the value of the output signal of the in-phase channel of the detector:

$$I_{QAMH} = U_1 + U_2 = \sqrt{2}A_m + \sqrt{2}\hat{n}_c(t) + \sqrt{2}\hat{n}_s(t), \tag{20}$$

and subtracting expression (19) from (18), we obtain the value of the output signal of the quadrature channel of the detector:

$$Q_{QAMH} = U_1 - U_2 = \sqrt{2}B_m + \sqrt{2}\hat{n}_c(t) - \sqrt{2}\hat{n}_s(t). \tag{21}$$

Assuming that the power of the noise processes $n^2(t)/2$ at the inputs of the in-phase and quadrature channels are equal, we can assume that $\hat{n}_s(t) = \hat{n}_c(t)\hat{n}(t)$.

From (20) and (21), it is clear that $\sqrt{2}\hat{n}(t)$ is the amplitude of the noise component of the AWGN in both the in-phase and quadrature channels. It can also be noted that this amplitude is nothing but the standard deviation $\sigma = \sqrt{2}\hat{n}(t)$ [13, p. 412] of the statistically independent processes $\hat{n}_s(t)$ and $\hat{n}_c(t)$, as mentioned above. In this case, we can write the sum for the noise component at the output of the corresponding channel of the synchronous detector after passing the low-pass filters in coherent detection (coherent averaging) as [13, pp. 412–415]:

$$\sigma + \sigma = \sqrt{2}n_c(t) + \sqrt{2}n_s(t) = \frac{\sqrt{2}\,\hat{n}(t)}{\sqrt{2}} = \hat{n}(t), \tag{22}$$

as in coherent averaging, $\sigma + \sigma = \frac{\sigma}{\sqrt{Z}}$ where Z is the number of realizations of the noise process (Z = 2 since there are two channels – in-phase and quadrature). In this case, the noise variance will also decrease $\sigma^2 = [\hat{n}(t)]^2$.

Taking into account that in (20) and (21) there is a coherent summation of noise in accordance with (22), then in this case, (20) and (21) will take the form:

ISSN 2076-2429 (print)
ISSN 2223-3814 (online)

$$I_{QAMH} = \sqrt{2}A_m + \hat{n}(t)\ , \tag{23}$$

$$Q_{QAMH} = \sqrt{2}B_m + \hat{n}(t)\ . \tag{24}$$

If we bring the amplitudes of signals (23) and (24) to the scale of amplitudes of modulating digital signals A_m and B_m, then we can finally write the expression for the demodulated QAMH signals as:

$$I_{QAMH} = A_m + \frac{\hat{n}(t)}{\sqrt{2}}\ , \tag{25}$$

$$Q_{QAMH} = B_m + \frac{\hat{n}(t)}{\sqrt{2}}\ . \tag{26}$$

Figure 3 shows the block diagram of the demodulator of the QAMH signal constructed in accordance with (16) – (21).

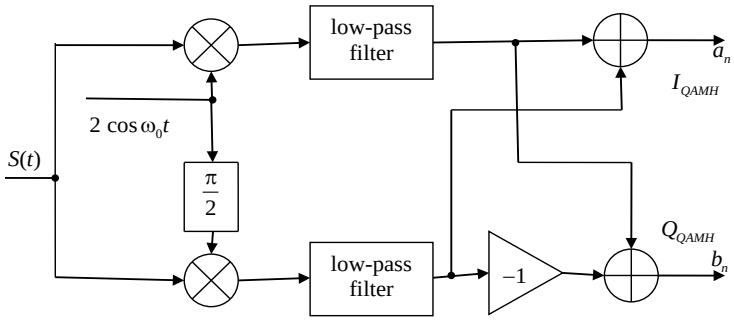

Fig. 3. Block diagram of the demodulator of the QAMH signal (low-pass filter)

At the synchronous detection of a conventional QAM signal in the in-phase channel of the demodulator, there will be a signal of the form [12]:

$$\begin{aligned} U_6 &= [A_m \cos(\omega_0 t) + B_m \sin(\omega_0 t) + n(t)/\sqrt{2}]\cdot 2\cos\omega_0 t = A_m \cos(\omega_0 t + \omega_0 t) + \\ &+ A_m \cos(\omega_0 t - \omega_0 t) + B_m \sin(\omega_0 t + \omega_0 t) + B_m \sin(\omega_0 t - \omega_0 t) + \sqrt{2}n(t)\cos\omega_0 t, \end{aligned} \tag{27}$$

and in the quadrature channel of the demodulator a signal of the form:

$$\begin{aligned} U_6 &= [A_m \cos(\omega_0 t) + b_n \sin(\omega_0 t) + n(t)/\sqrt{2}]\cdot 2\sin\omega_0 t = A_m \sin(\omega_0 t + \omega_0 t) + \\ &+ A_m \sin(\omega_0 t - \omega_0 t) + B_m \cos(\omega_0 t - \omega_0 t) - B_m \cos(\omega_0 t + \omega_0 t) + \sqrt{2}\, n(t)\sin\omega_0 t. \end{aligned} \tag{28}$$

We will also assume that the characteristics of the low-pass filters of the synchronous detectors of the QAM and QAMH signals are identical. As a consequence, it is also assumed that the powers of the noise processes in the in-phase and quadrature channels after filtering will be equal, i.e. $\hat{n}_s(t) = \hat{n}_c(t) = \hat{n}(t)$, where $\sqrt{2}\hat{n}_c(t)$ is the amplitude of the noise (process) $\sqrt{2}n(t)\cos\omega_0 t$ after filtering in the in-phase channel and $\sqrt{2}\hat{n}_s(t)$ is the amplitude of the noise (process) $\sqrt{2}n(t)\sin\omega_0 t$ after filtering in the quadrature channel.

After the low-pass filtering of signals (27) and (28), the low-pass filter with a cutoff frequency $\Omega = \frac{1}{T}$ will select the signals in the in-phase and quadrature channels, respectively:

$$I_{QAM} = A_m + \sqrt{2}\ \hat{n}(t)\ , \tag{29}$$

$$Q_{QAM} = B_m + \sqrt{2}\hat{n}(t)\ . \tag{30}$$

The energy gain of the QAMH modulation in comparison with the QAM modulation can be defined as the ratio of signal-to-noise (*S/N*) values in the communication channel for the QAMH and QAM signals (at equal amplitudes A_m and B_m. Taking into account the equality of the amplitudes of the QAMH signals in (25) and (26) and the QAM signals in (29) and (30), the energy gain when using QAMH signals can be defined as:

$$E = \frac{(S/N)_{QAMH}}{(S/N)_{QAM}} = \frac{\frac{a_n}{\frac{\hat{n}(t)}{\sqrt{2}}}}{\frac{a_n}{\sqrt{2}\,\hat{n}(t)}} = 2\,. \qquad (31)$$

5. Results of simulation modelling

The result obtained in (31) corresponds to the total energy gain when applying the QAMH modulation by a factor of two (or $20\lg 2 = 6\,dB$ on a logarithmic scale) compared to the signal with the QAM modulation. It should be noted that 3dB (out of 6dB) of the energy gain when using the QAM signal is provided by coherent summation of signals in the formation of signals (25) and (26) (which is not the case when performing demodulation of the QAMH signal).

Another 3dB is provided due to the increased amplitude at the output of the QAMH signal detector $\sqrt{2}$ times compared to the QAMH signal, as can be seen from (23) and (24).

Figure 4 shows the dependence of BER (Bit Error Rate) on the signal-to-noise ratio (*S*/*N*) for signals with QAMH 256, which was obtained as a result of simulation modelling when this signal passes through the communication channel with the AWGN.

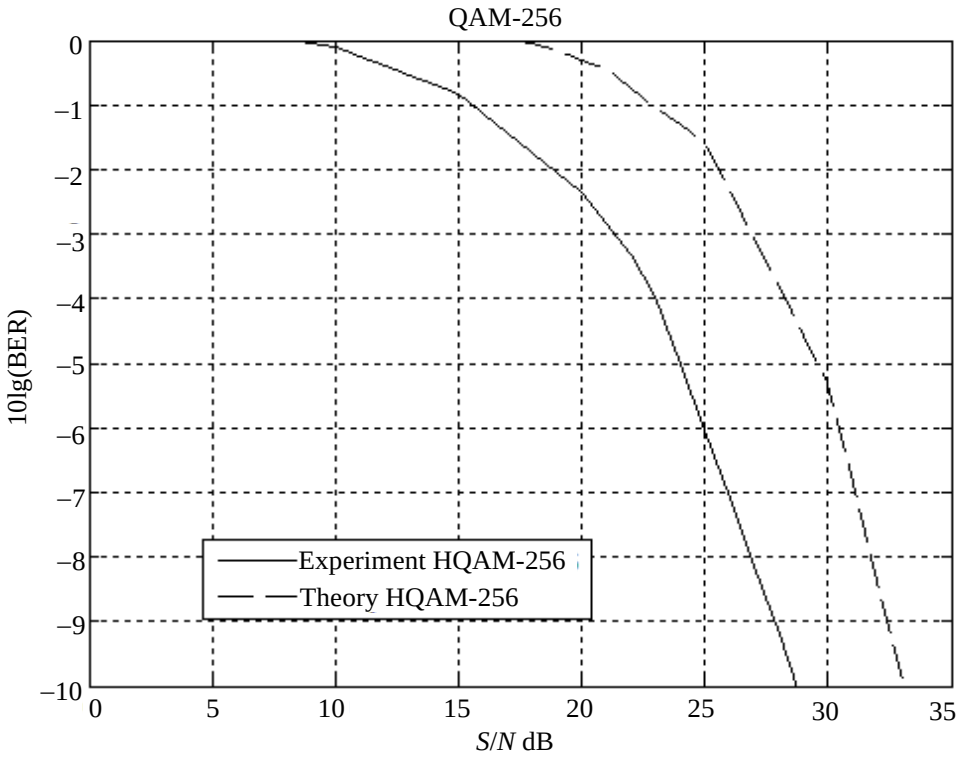

Fig. 4. Dependence of the probability of an incorrectly received symbol for QAMH 256 on the signal-to-noise ratio

Figure 4 also shows the theoretical BER limit for the QAM256 signal in accordance with [8, p. 237], which shows a good agreement between theory and experiment.

The energy gain when using the QAMH signals is equal to two compared to the use of the QAM signals, which follows from (31). In this case, we can write the relation for the noise power when using the QAMH signals in the form:

$$N_{QAMH\,b} = \left(\frac{\hat{n}(t)}{2}\right)^2 = \frac{N_0}{4}, \qquad (32)$$

where: N_0 is, in this case, the noise power at the output of the synchronous detector when demodulating the QAMH signal.

ISSN 2076-2429 (print)
ISSN 2223-3814 (online)

The expression for determining the upper limit of the probability of an incorrectly received symbol error for a QAM signal [8, p. 237] is:

$$P_{QAM\ b} \le 4Q\left(\sqrt{\frac{3\cdot k\cdot E_{bcp}}{(M-1)N_0}}\right), \tag{33}$$

where k is the number of bits in the symbol, E_{bcp} is the average energy per 1 bit, $M = 2^k$, N_0 is the noise power. Substituting the value $N_{QAMH} = \frac{N_0}{4}$ in (32), we obtain the expression for calculating the upper bound of the erroneously received symbol for the QAM signal:

$$P_{QAMH\ b} \le 4Q\left(\sqrt{\frac{3\cdot k\cdot E_{bcp}}{(M-1)\frac{N_0}{4}}}\right) = 4Q\left(\sqrt{\frac{12\cdot k\cdot E_{bcp}}{(M-1)N_0}}\right). \tag{34}$$

Figure 5 shows a good match between the curve for the theoretical result according to (34) and the curve of the result obtained from the simulation.

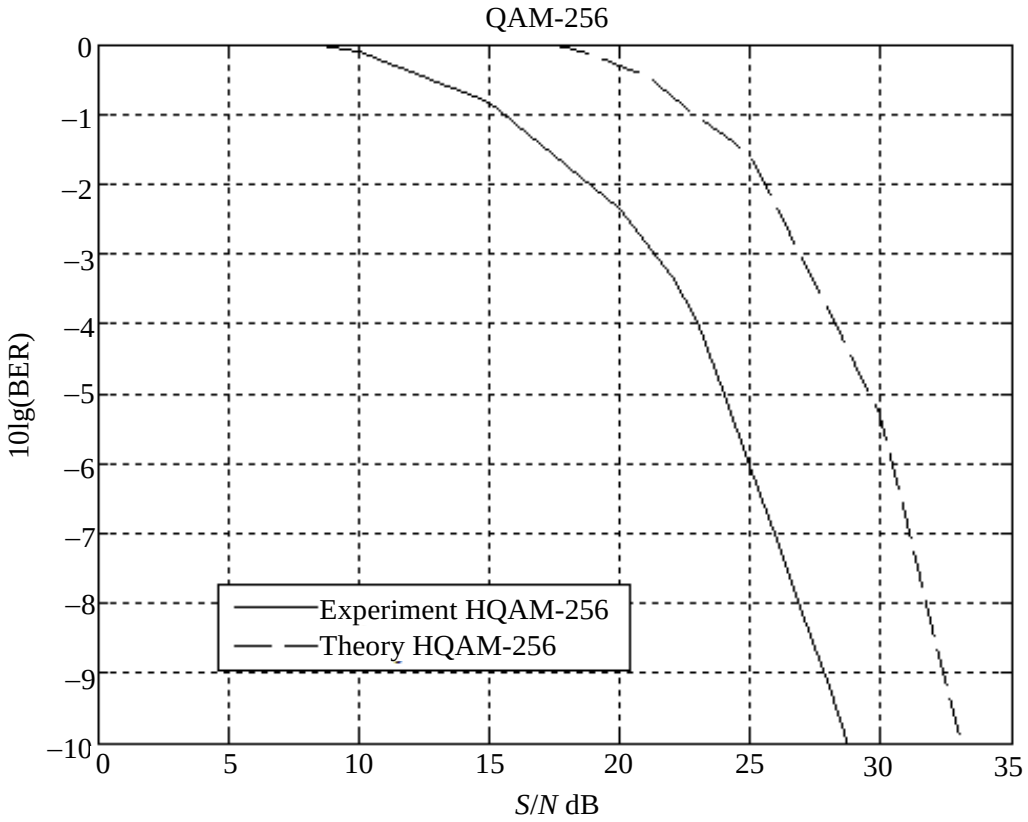

Fig. 5. Dependence of the probability of an incorrect symbol for HQAM 256 on the signal-to-noise ratio and the calculated theoretical value for HQAM 256 according to (34)

A slight discrepancy between the curves in Figure 5 is explained by the fact that the modelling uses pseudorandom sequences of finite length. Figure 6 shows the scatter diagrams for QAMH 256 and QAM 256 at different values of the signal-to-noise ratio (S / N).

These diagrams show that the signal from QAMH 256 is better separated than the signal from KAM 256, which confirms the better noise immunity of these signals. As can be seen from Figure 6, with a signal-to-noise ratio of 20 dB, it is possible to divide the QAMH 256 signal, at the same time, the BER value is equal to 10^{-3} (Figure 4). Under the same conditions (signal-to-noise ratio of 20 dB), the QAM 256 signal cannot be separated, while the BER error value for the QAM signal will be within 10^{-1}.

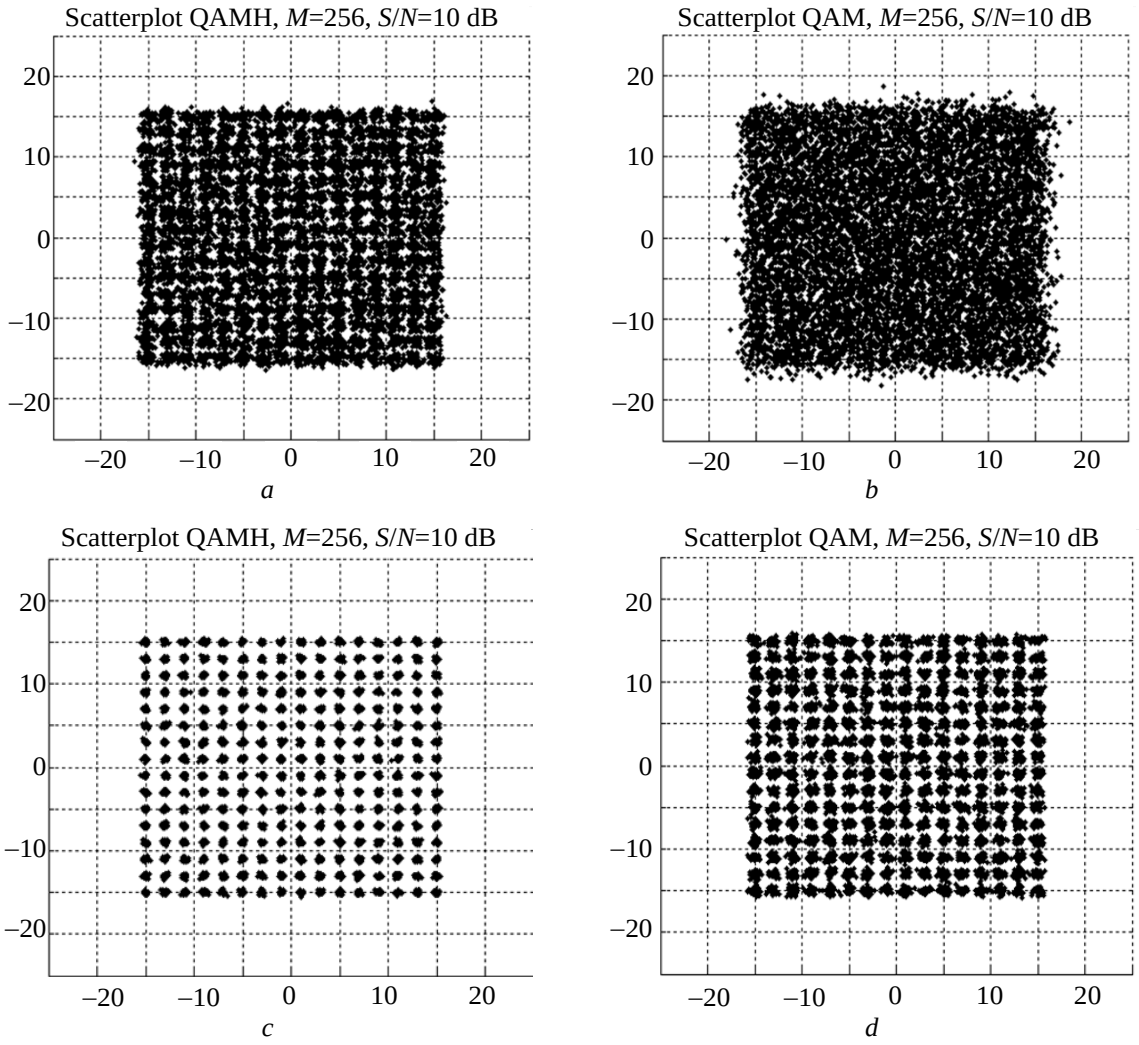

Fig. 6. Signal scattering diagrams of QAMH 256 (left) and QAM 256 (right) at different values of signal-to-noise ratio: *a* – 10dB for QAMH 256; *b* – 10dB for QAM 256; *c* – 20dB for QAMH 256; *d* – 20dB for QAM 256

6. Conclusion

The use of signals with QAMH modulation allows to increase the signal resistance to noise in the communication channel by 6 dB compared to the use of QAM signals and to reduce the value of the average energy per bit by half. In modern communication systems, QAM signals are used mainly for line-of-sight systems where the communication range is limited. In such systems, there is no need to increase the communication range, which allows to reduce the power of the QAMH transmitter signal by 6 dB (i.e., 3.98 times) while maintaining the distance, receiver parameters and communication quality, as shown in [7].

The possibility of reducing the power of the QAMH signal transmitter leads, in turn, to a reduction in power consumption by the communication system, since the transmitter consumes approximately 90…95% of the total power consumed by the communication system. This is especially important when operating on battery power. The reduced power consumption of transmitters that generate the QAMH signal also makes it possible in many cases to significantly reduce the size of the transmitter. If it is necessary to double the communication range (which is substantiated in [7]), the power of the QAMH signal transmitter will be used the same as the power of the QAM signal transmitter (while maintaining the receiver sensitivity), but the communication range will double.

Література

1. Alonso A. M., Miyahara M., Matsuzawa A. A 12.8-ns-Latency DDFS MMIC With Frequency, Phase, and Amplitude Modulation in 65-nm CMOS. *IEEE Journal of Solid-State Circuits*. 2018. Vol. 53, Issue 10. P. 2840–2849.

ISSN 2076-2429 (print)
ISSN 2223-3814 (online)

2. Absolute Amplitude Differential Phase Spatial Modulation and Its Non-Coherent Detection Under Fast Fading Channels / Yu D., Yue G., Liu A. et al. *IEEE Transactions on Wireless Communications*. 2020. Vol. 19, Issue 4. P. 2742–2755.
3. Neshaastegaran P., Banihashemi A. H. Log-Likelihood Ratio Calculation for Pilot Symbol Assisted Coded Modulation Schemes With Residual Noise. *IEEE Transactions on Communications*. 2019. Vol. 67, Issue 5. P. 3782–3790.
4. High-Speed Reconfigurable Free-Space Optical Interconnects with Carrierless-Amplitude-Phase Modulation and Space-Time-Block Code / Wang K., Lim C., Wong E. et al. *Journal of Lightwave Technology*. 2019. Vol. 37, Issue 2. P. 627–633.
5. A Survey on Higher-Order QAM Constellation: Technical Challenges, Recent Advances, and Future Trends / Singya P. K., Shaik P., Kumar N. et al. *IEEE Open Journal of the Communications Society*. 2021. Vol. 2. P. 617–655.
6. Hati A., Nelson C. W. A Simple Optimization Method for Generating High-Purity Amplitude and Phase Modulation. *IEEE Transactions on Instrumentation and Measurement*. 2022. Vol. 71. DOI: 10.1109/TIM.2022.3186367.
7. Kokhanov A. B. Hartley's Amplitude, Balanced and Single Band Modulations. *Radioelectronics and Communications Systems*. 2022. Vol. 65, № 6. P. 293–304. DOI: 10.3103/S0735272722060036.
8. Прокис Дж. Цифровая связь : пер. с англ. / Дж. Прокис ; под ред. Д. Д. Кловского. М. : Радио и связь, 2000. 800 с. ISBN 5-256-01434-X.
9. Галкин, В. А. Цифровая мобильная связь : учеб. пособ. для вузов. 2-е изд., перераб. и доп. М. : Горячая линия–Телеком, 2012. 592 с.
10. Коханов А. Б. Исследование зависимости появления ошибок сигнала с квадратурной модуляцией Хартли в зависимости от отношения сигнал-шум. *International scientific-practical conference. Science, Education and Technology. Book of abstracts*. Bila Tserkva, 2024. P. 36–37.
11. Левин Б. Р. Теоретические основы статистической радиотехники. 3-е изд., перераб. и доп. М. : Радио и связь, 1989. 656 с. ISBN 5-256-00264-3.
12. Сергиенко А. Б. Цифровая обработка сигналов. СПб. : Питер, 2003. 604 с.
13. Лайонс Р. Цифровая обработка сигналов : второе изд. М. : БИНОМ-ПРЕСС, 2011. 656 с.

References

1. Alonso, A. M., Miyahara, M., & Matsuzawa, A. (2018). A 12.8-ns-Latency DDFS MMIC With Frequency, Phase, and Amplitude Modulation in 65-nm CMOS. *IEEE Journal of Solid-State Circuits*, *53*(10), 2840–2849.
2. Yu, D., Yue, G., Liu, A., & Yang, L. (2020). Absolute Amplitude Differential Phase Spatial Modulation and Its Non-Coherent Detection Under Fast Fading Channels. *IEEE Transactions on Wireless Communications*, *19*(4), 2742–2755.
3. Neshaastegaran, P., & Banihashemi, A. H. (2019). Log-Likelihood Ratio Calculation for Pilot Symbol Assisted Coded Modulation Schemes With Residual Noise. *IEEE Transactions on Communications*, *67*(5), 3782–3790.
4. Wang, K., Lim, C., Wong, E., Alameh, K., Kandeepan, S., & Skafidas, E. (2019). High-Speed Reconfigurable Free-Space Optical Interconnects with Carrierless-Amplitude-Phase Modulation and Space-Time-Block Code. *Journal of Lightwave Technology*, *37*(2), 627–633.
5. Singya, P. K., Shaik, P., Kumar, N., Bhatia, V., & Alouini, M.-S. (2021). A Survey on Higher-Order QAM Constellation: Technical Challenges, Recent Advances, and Future Trends. *IEEE Open Journal of the Communications Society*, *2*, 617–655.
6. Hati, A., & Nelson, C. W. (2022). A Simple Optimization Method for Generating High-Purity Amplitude and Phase Modulation. *IEEE Transactions on Instrumentation and Measurement*, *71*. DOI: 10.1109/TIM.2022.3186367.
7. Kokhanov, A. B. (2022). Hartley's Amplitude, Balanced and Single Band Modulations. *Radioelectronics and Communications Systems*, *65*(6), 293–304. DOI: 10.3103/S0735272722060036.
8. Prokis, J. (2000). *Digital communication* (D. D. Klovsky, Ed.; Translated from English). Radio i sviaz.
9. Galkin, V. A. (2012). *Digital mobile communication* (2nd ed., rev. and enl.). Goryachaya liniya–Telekom.

10. Kokhanov, A. B. (2024). A study of the dependence of the appearance of errors in a Hartley quadrature modulated signal on the signal-to-noise ratio. In *Science, Education and Technology: Book of abstracts* (pp. 36–37). International scientific-practical conference. Bila Tserkva.
11. Levin, B. R. (1989). *Theoretical foundations of statistical radio engineering* (3rd ed., rev. and enl.). Radio i sviaz.
12. Sergienko, A. B. (2003). *Digital signal processing*. St. P.: Piter.
13. Lyons, R. (2011). *Understanding digital signal processing* (2nd ed.). M.: BINOM-PRESS.

Коханов Олександр Борисович; Aleksandr Kokhanov, ORCID: https://orcid.org/0000-0002-7197-6380

Received February 03, 2025
Accepted March 18, 2025